Phycologia (2007) Volume 46 (2), 151–159 Published 1 March 2007

Resolution of codominant phytoplankton species in a eutrophic lake using synchrotron-based Fourier transform infrared spectroscopy

A.P. DEAN[1]*, M.C. MARTIN[2] AND D.C. SIGEE[1]

[1]*School of Biological Sciences, University of Manchester, 3.614 Stopford Building, Oxford Road, Manchester M13 9PT, UK*
[2]*Advanced Light Source Division, Lawrence Berkeley National Laboratory, 1 Cyclotron Road, Berkeley, CA 94720-8226*

A.P. DEAN, M.C. MARTIN AND D.C. SIGEE. 2007. Resolution of codominant phytoplankton species in a eutrophic lake using synchrotron-based Fourier transform infrared spectroscopy. *Phycologia* 46: 000–000.

Synchrotron-based Fourier-transform infrared (FTIR) microspectroscopy was used to distinguish micropopulations of the codominant algae *Microcystis aeruginosa* (Cyanophyceae) and *Ceratium hirundinella* (Dinophyceae) in mixed phytoplankton samples taken from the water column of a stratified eutrophic lake (Rostherne Mere, UK). FTIR spectra of the two algae showed a closely similar sequence of 10 bands over the wave-number range 4000–900 cm^{-1}. These were assigned to a range of vibrationally active chemical groups using published band assignments and on the basis of correlation and factor analysis. In both algae, intracellular concentrations of macromolecular components (determined as band intensity) varied considerably within the same population, indicating substantial intraspecific heterogeneity. Interspecific differences were separately analysed in relation to discrete bands and by multivariate analysis of the entire spectral region 1750–900 cm^{-1}. In terms of discrete bands, comparison of individual intensities (normalised to amide 1) demonstrated significant (99% probability level) differences in relation to six bands between the two algal species. Key interspecific differences were also noted in relation to the positions of bands 2, 10 (carbohydrate) and 7 (protein) and in the 3-D plots derived by principal component analysis (PCA) of the sequence of band intensities. PCA of entire spectral regions showed clear resolution of species in the PCA plot, with indication of separation on the basis of protein (region 1700–1500 cm^{-1}) and carbohydrate (region 1150–900 cm^{-1}) composition in the loading plot. Hierarchical cluster analysis (Ward algorithm) of entire spectral regions also showed clear discrimination of the two species within the resulting dendrogram.

KEY WORDS: *Ceratium,* FTIR, *Microcystis,* Phytoplankton

INTRODUCTION

The ability to determine the chemical and molecular composition of individual algal cells and colonies within mixed microalgal samples has considerable importance for phytoplankton ecology, providing potential information on chemical diversity within micropopulations, taxonomic differentiation at the species and subspecies level and physiological responses of single species to ecological factors such as light and nutrient stress. A range of high-resolution techniques are now available to carry out such *in situ* analysis, including X-ray microanalysis (Sigee & Levado 2000), use of molecular probes (Litaker *et al.* 2003), chemiluminescence (Villareal & Lipschultz 1995) and Fourier-transform infrared (FTIR) spectroscopic analysis (Sigee *et al.* 2002). Of these techniques, FTIR spectroscopy has particular potential for phytoplankton analysis (Sacksteder & Barry 2001) since it is able to provide simultaneous information on a wide range of molecular groups within individual microalgae. The use of synchrotron radiation as the IR source has the added benefit of allowing high-quality spectra to be obtained from very small sample areas, facilitating the analysis of small cells that are common components of the freshwater phytoplankton.

In recent years, phycological use of FTIR spectroscopy has been particularly in relation to cultured algal cells. The technique has been used, for example, to investigate the physiological effects of nitrogen deprivation on the diatom *Chaetoceros* (Giordano *et al.* 2001) and to study nutrient stress-related changes in various blue-green algae and diatoms (Stehfast *et al.* 2005). Heraud *et al.* (2005) have pioneered the use of FTIR with living cells, showing a redistribution of macromolecular pools in relation to nutrient stress in the green alga *Micrasterias.* In the field of taxonomy, Kansiz *et al.* (1999) have used of FTIR spectroscopy to discriminate between blue-green algal strains.

Although FTIR spectroscopy has been widely used in a laboratory context, there have been relatively few studies on environmental samples. Synchrotron-based FTIR studies by Sigee *et al.* (2002) showed that high-quality FTIR spectra could be readily obtained from air-dried lake phytoplankton samples deposited on a reflectance slide, providing molecular information on the target species (*Pediastrum duplex*) in relation to nucleic acid, lipid, carbohydrate and protein content. FTIR analysis of a mixed phytoplankton samples from the same lake (Dean & Sigee 2006) showed clear molecular differentiation of the blue-green algae *Aphanizomenon flos-aquae* and *Anabaena flos-aquae,* with further separation of *Aphanizomenon* into epilimnion and hypominion subsets.

The present study is one of a series of projects designed to test the applicability of FTIR analysis to freshwater phytoplankton in defined ecological situations. This investigation uses synchrotron-based FTIR spectroscopy for molecular

* Corresponding author (andrew.dean@manchester.ac.uk).

comparison of *Microcystis aeruginosa* (Kŧz emend Elenkin) and *Ceratium hirundinella* (O.F. Mull.), present as codominant algae within the late summer bloom of a eutrophic lake.

MATERIAL AND METHODS

Collection and processing of samples

Samples were collected from Rostherne Mere (Cheshire, UK) on 24 August 2001. Trawl net samples of phytoplankton were collected from the epilimnion in the central part of the lake using a 63-μm mesh size phytoplankton net. Within 1 h of collection, 10-ml aliquots were resuspended in deionised water and droplets of the phytoplankton suspension deposited on 'Low-e' reflectance slides (Kevley Technologies). Samples were subsequently air-dried in a laminar flow at room temperature and stored in a desiccator until analysis.

Integrated samples (0–5-m depth) of lake water were collected using a flexible hose at three separate sites on the lake and used for the determination of inorganic nutrient concentrations and chlorophyll *a* (Chl *a*) concentration and species counts. Mean biovolume for individual algal cells was calculated from the geometrical formulas in Wetzel & Likens (2000) and Willen (1976). *Microcystis* colony biovolume was calculated by multiplying cell volume by the number of cells in an average colony, estimated using the equation given in Reynolds & Jaworski (1978).

The limit of light penetration at each site was measured using a Secchi disk.

Infrared analysis

Synchrotron-dependent infrared analysis was carried out at the Advanced Light Source (Lawrence Berkeley National Laboratory) on Beamline 1.4.3. The FTIR instrumentation for the beam line consists of a Nicolet 760 FTIR bench and a Spectra-Tech Nic-Plan IR microscope. The use of a high-intensity synchrotron source allowed very small apertures to be employed while maintaining an adequate signal-to-noise ratio. Spectra were collected using a 10-μm-square aperture and were collected over the wave-number range 4000–650 cm $^{-1}$. Spectral resolution of the mercury cadmium telluride (MCT) detector was 4 cm^{-1} with 64 coadded scans. Infrared absorption spectra were collected from clear field (background) and from colonies of algae (see Fig. 2), and a ratio was obtained of the sample to background spectrum. Specimens were examined and analysed in the dry state, with no mounting medium or coverslip.

Phytoplankton samples were initially examined by bright-field microscopy, and 20 individual colonies of *Microcystis* and 20 cells of *Ceratium* were randomly selected within the mixed phytoplankton population for analysis (one spectrum per colony/cell). Spectral absorption bands were identified in relation to published information. Supporting information on band assignments was also obtained by analysis of a range of pure biochemical standards (protein, nucleic acid, fatty acid and soluble carbohydrate) as detailed in Sigee *et al.* (2002).

SPECTRAL ANALYSIS: Manipulation of FTIR spectra was carried out using Nicolet OMNIC software (Nicolet Ltd). Spectra were baseline-corrected using the automatic baseline correct algorithm and were normalised to amide I.

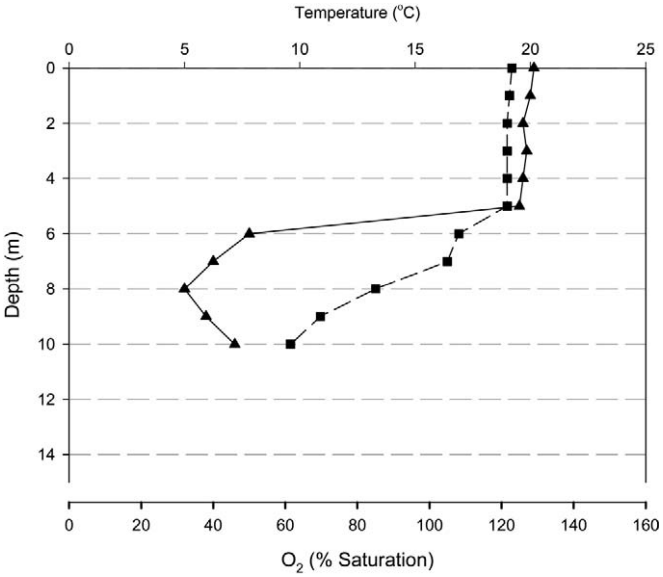

Fig. 1. Depth profiles of temperature and oxygen concentration. Depth profiles of temperature (■) and oxygen concentration (▲) indicate stratification, with an epilimnion extending down to 5 m. Measurements were taken at 1-m intervals.

Two approaches were carried out in relation to quantitative analysis. Firstly, the intensities of each discrete band (i.e. 10 data points per spectrum) were recorded. These data were used to study the relationships between individual bands within species using correlation analysis and principal component analysis, as well as investigating interspecific differences in terms of band intensities. Statistical analysis on band intensities was carried out using EXCEL and SPSS software.

The second approach was the use of multivariate analysis to compare whole spectra over the wave-number range 1750–900 cm^{-1}, the region in which the majority of the molecular information lies, resulting in 442 data points per spectrum. Principal component analysis (PCA) was used to compare spectra from the two algal species using scores plots to visualise the data, with each point on the plot representing an individual spectrum. This allowed the clustering of data sets to be visualised. Loading plots were then generated that showed the regions of the spectra (e.g. protein, carbohydrate) responsible for the observed separation. PCA was carried out in MATLAB (The MathWorks Inc.). Hierarchical cluster analysis was carried out in SPSS 11.5.

RESULTS

Conditions within the water column

At the time of sampling, Rostherne Mere was undergoing a pronounced algal bloom. The high phytoplankton biomass was reflected in the high Chl *a* concentration of 71 μg l^{-1} and a Secchi depth of 1.0 m. The high pH of 9.0 suggested high photosynthetic activity, as did the high-percentage oxygen saturation, which was supersaturated in the epilimnion (Fig. 1). Concentrations of nutrients were low, with soluble reactive phosphorus undetectable and nitrates present at 0.01 mg l^{-1}.

The mixed phytoplankton population was dominated

Table 1. Species composition at time of sampling.[1]

	Cell/colony count (no. ml^{-1})	Mean biovolume per cell/ colony ($\mu m^3 \times 10^3$)	Total species biovolume ($\mu m^3 \times 10^6$)	Percentage of total biovolume
Microcystic aeruginosa	120	77.1	9.252	79.4
Ceratium hirundinella	51	41.4	2.111	18.1
Aphanizomenon flosaquae	51	1.52	0.078	0.7
Staurastrum sp.	57	3.1	0.177	1.5
Scenedesmus quadricauda	20	0.16	0.003	0.03
Cryptomonas erosa	37	1.05	0.039	0.33

[1] Species counts are the mean value from three integrated (epilimnion) samples obtained from different sites on the lake.

throughout the water column by colonies of the blue-green alga *Microsystis aeruginosa*, together with the dinoflagellate *C. hirundinella* (Table 1). Within the epilimnion, these two algae accounted for 79% and 18%, respectively, of the total phytoplankton biovolume, with less than 3% occupied by other species. Other algae present included the blue-green alga *Aphanizomenon flos-aquae*, the green algae *Staurastrum* sp. and *Scenedesmus quadricauda* and the cryptomonad *Cryptomonas* spp.

Band assignments

Under the light microscope, air-dried preparations of mixed phytoplankton samples showed typical images of the two major species (Fig. 2). *Microcystis aeruginosa* appeared as large irregular colonies and *C. hirundinella* as single cells with prominent spines. Spectral analysis was carried out over 10 × 10-μm areas of specimen (Fig. 3), generating infrared absorption spectra that were closely similar for *Microcystis* and *Ceratium* (Fig. 4), each containing 10 clear bands over the wave-

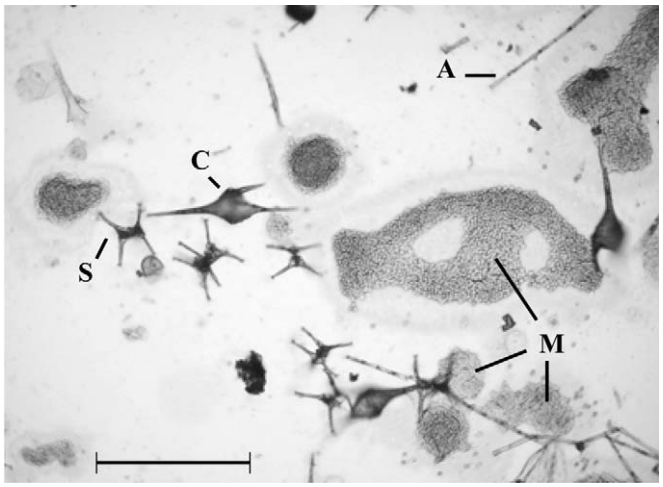

Fig. 2. Light microscope images of air-dried mixed phytoplankton sample. (2a) Low-power view showing the dominant algae *Microcystis* (M) and *Ceratium* (C) plus *Aulacoseira* (A) and *Staurastrum* (S). Scale − 200 μm.

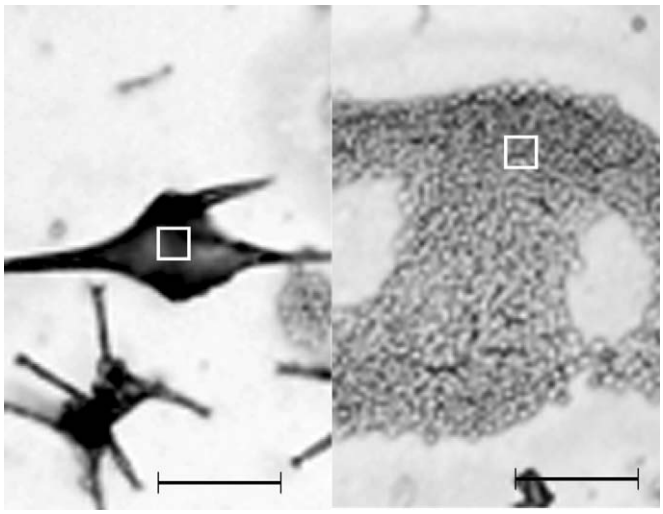

Fig. 3. Detail from Fig. 2, showing the position of the 10-μm-square probe area (region of analysis) in *Ceratium* and *Microcystis*, respectively. Scale − 50 μm.

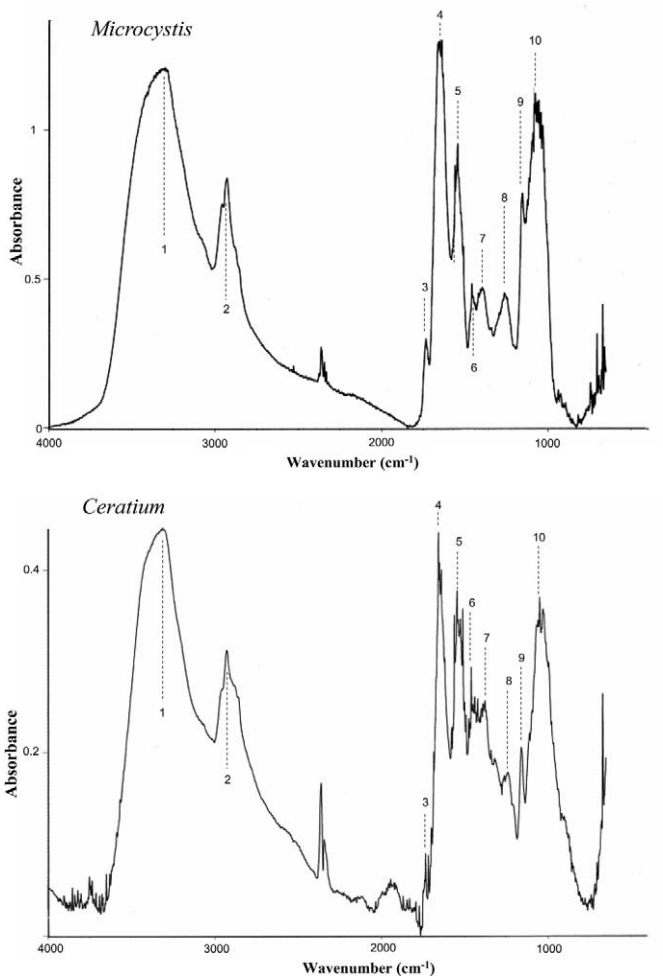

Fig. 4. Infrared absorption spectra from an air-dried colony of *Microcystis* and a single cell of *Ceratium*. Band assignments are given in Table 2.

Table 2. Assignment of bands formed in FTIR specra from *Microcystis* and *Ceratium*.[1]

	Main peak (*Ceratium* in brackets)	Typical band assignment from the literature	Attribution in this study (see discussion)
1	3303 (3332)	water υ(O-H) stretching protein υ(N-H) stretching (amide A)	carbohydrate
2	2929 (2919)	lipid $\delta_{as}(CH_2)$ of methylene, primarily from lipids	carbohydrate
3	1734	lipid υ(C=O) of ester functional groups primarily from lipids and fatty acids	lipid
4	1655 (1653)	protein mainly υ(C=O) stretching of amides associated with proteins	protein
5	1541	protein amide II band δ(N-H) of amides associated with proteins	protein
6	1456	protein and lipid $\delta_{as}(CH_2)$ and $\delta_{as}(CH_3)$ bending of methyl	protein
7	1398 (1373)	protein $\delta_s(CH_2)$ and $\delta_s(CH_3)$ bending of methyl CARBOXYLIC ACID υ_s(C-O) of COO^- groups of carboxylates	protein
8	1244 (1255)	nucleic acid υ_{as}(>P=O) stretching of phosphodiester backbone of nucleic acid	nucleic acid or stored P
9	1152 (1156)	carbohydrate υ(C-O-C) of polysaccharides	carbohydrate
10	1081 (1063) In some spectra bands also seen at ≈1050 and ≈1030	carbohydrate υ(C-O-C) of polysaccharides nucleic acid υ_s(>P=O) stretching of phosphodiesters	carbohydrate

[1] Band assignments based on Benning *et al.* (2004), Giordano *et al.* (2001), Keller (1986), Naumann *et al.* (1996), Stuart (1997) and Wong *et al.* (1991).

number range 4000–900 cm^{-1}. Table 2 shows the assignments of the bands based on literature sources. As individual bands may have contributions from a number of molecular groups representing different macromolecular components, correlation and PC analysis has been used to aid in band assignment, and this has led to some band assignments differing from those typically given in the literature, the rationale for which is given in the discussion. Bands are attributed to a range of vibrational states in lipids, proteins, nucleic acids (plus other phosphorus-containing compounds) and carbohydrate (Table 2). CO_2 contributed a consistent extraneous band with a peak at wave number 2362 cm^{-1} that was excluded from any further analysis.

Intraspecific heterogeneity

Intraspecific variation in band intensity gives a measure of population heterogeneity, indicating how intracellular concentrations of macromolecular components varied between algae taken from the same population. Table 3 shows band intensities for each species, together with the coefficient of variation (CV). In *Ceratium*, band 5 (amide II) showed the smallest coefficient of variation—probably as a result of its being normalised to band 4 (amide I). Bands 1, 2, 9 and 10 showed the highest variation (CV > 30%), with band 10 having a CV of 47%; other bands had CVs of between 18% and 26%. In *Microcystis*, band 5 again showed the smallest coefficient of variation (8%). Other bands in this alga showed less variation than in *Ceratium*, with CVs of between 22% and 36%.

Table 3. Comparison of band intensities. For each algal species, mean band intensities are shown as normalised data referenced to band 4 (n = 20). Comparison of normalised means, Mann-Whitney Test. Bands 1–3, 5–6 and 10 are significantly different at the 99% level of probability.[1]

	Microcystis		*Ceratium*		
Band	Mean	CV	Mean	CV	Significance
1	0.994	23	1.483	37	0.000**
2	0.604	27	0.868	32	0.001**
CO_2	*0.228*	*46*	*0.740*	*34*	*0.000***
3	0.149	36	0.287	26	0.000**
4					
5	0.722	8	0.804	10	0.002**
6	0.392	22	0.594	18	0.000**
7	0.404	28	0.579	20	0.799
8	0.320	32	0.331	25	0.640
9	0.529	33	0.680	33	0.018
10	0.696	28	1.483	47	0.000**

[1] For each algal species (n = 20), mean band intensities are shown as normalised data referenced to amide I. Comparison of normalised means used Mann-Whitney test. Bands 1–3, 5–6 and 10 are significantly different at the 99% level of probability.

Comparison of species

ANALYSIS OF DISCRETE BANDS: This involved statistical comparisons between the two species in relation to individual band intensities, band positions, and principal component analysis (PCA) of the band sequence.

Comparison of band intensities (normalised to amide 1) using the Mann–Whitney test (Table 3) demonstrated major differences in relative band intensities between the two algal species, with bands 1, 2, 3, 5, 6 and 10 showing significant differences between the algae at the 99% significance level. Band 9 showed a significant difference at the 95% significance level. Only bands 7 and 8 did not show any significant difference.

The nonparametric (Spearman) correlations shown in Table 4 (99% probability level) reveal high levels of correlation between certain bands. In *Microcystis*, bands 1 and 2 show a strong correlation. Bands 2, 9 and 10 show positive correlations with each other, as do bands 6, 7 and 8. In *Ceratium*, bands 1, 2 and 10 are correlated. Bands 6 and 7 are correlated with each other and with band 9. Bands 9 and 10 are strongly correlated.

Although the two algal species had a similar pattern of bands, individual band positions showed interspecific differences (Table 5). The average position of bands 1, 2, 7, 8 and 10 in *Microcystis* and *Ceratium* differed by more than the 4 cm^{-1} resolution of the instrument. However, variation was

Table 4. Nonparametric correlations between band intensities in *Microcystis* and *Ceratium*.[1]

Band	1	2	3	4	5	6	7	8	9	10
1	—	**0.805**								
2	0.905	—							**0.602**	**0.600**
3			—							
4				—						
5					—					
6						—	**0.971**	**0.726**		
7						0.728	—	**0.750**		
8								—		
9						0.603	0.781		—	**0.920**
10	0.654	0.725							0.727	—

[1] Correlation coefficients (significant at 99% probability level) are shown for Spearman (nonparametric) analysis (n = 20). *Microcystis* – bold type upper half of table; *Ceratium* – light type lower half of table.

seen between spectra, and only three bands (2, 7 and 10) were significantly different at the 99% probability levels.

PCA analysis of the sequence of band intensities showed distinctive three-dimensional plots for the two algae (Fig. 5). For *Microcystis*, three factors were extracted. PC1 accounted for 30% of total variance and consisted of bands 6, 7 and 8, while PC2 (29%) consisted of bands 3, 5, 9 and 10 and PC3 (28%) bands 1, 2 and 10. For *Ceratium*, PC1 (38%) consists of bands 1, 2, 9 and 10; PC2 (27%) bands 3, 6, 7 and 9; and PC3 (18%) bands 5 and 8.

MULTIVARIATE ANALYSIS OF SPECTRAL REGION 1750–900 CM^{-1}: PCA and hierarchical cluster analysis (HCA) were carried out for the combined set of spectra (20 *Microcystis*, 20 *Ceratium*) over the 1750–900 cm^{-1} wave-number region. Variation within this data set was determined by two statistical factors—principal component 1 (PC1–49% of variability) and principal component 2 (PC2–30% of variability). The PC scores plot of PC1 against PC2 (Fig. 6) shows a clear separation between the two algae, with individual spectra separated into two major clusters.

The regions of the spectra that are responsible for the separation of groups in PCA plots can be investigated using loading plots. These show which are the most important wave numbers in separating the groups along each PC, with the magnitude of the loading being a measure of the importance of that wave number to the separation. Wave numbers with zero loading represent unimportant features. The loading plot (Fig. 6) shows that along PC1, the main separation between species occurs within the region 1700–1500 cm^{-1}, associated with protein, and 1150–900 cm^{-1}, associated with carbohydrate.

Figure 7 shows the results from the hierarchical cluster analysis (Ward algorithm) using Euclidian distance squared as the measure of similarity. The dendrogram shows the two species to be clearly separated on the basis of their spectra, with *Ceratium* spectra occurring as a single cluster and *Microcystis*

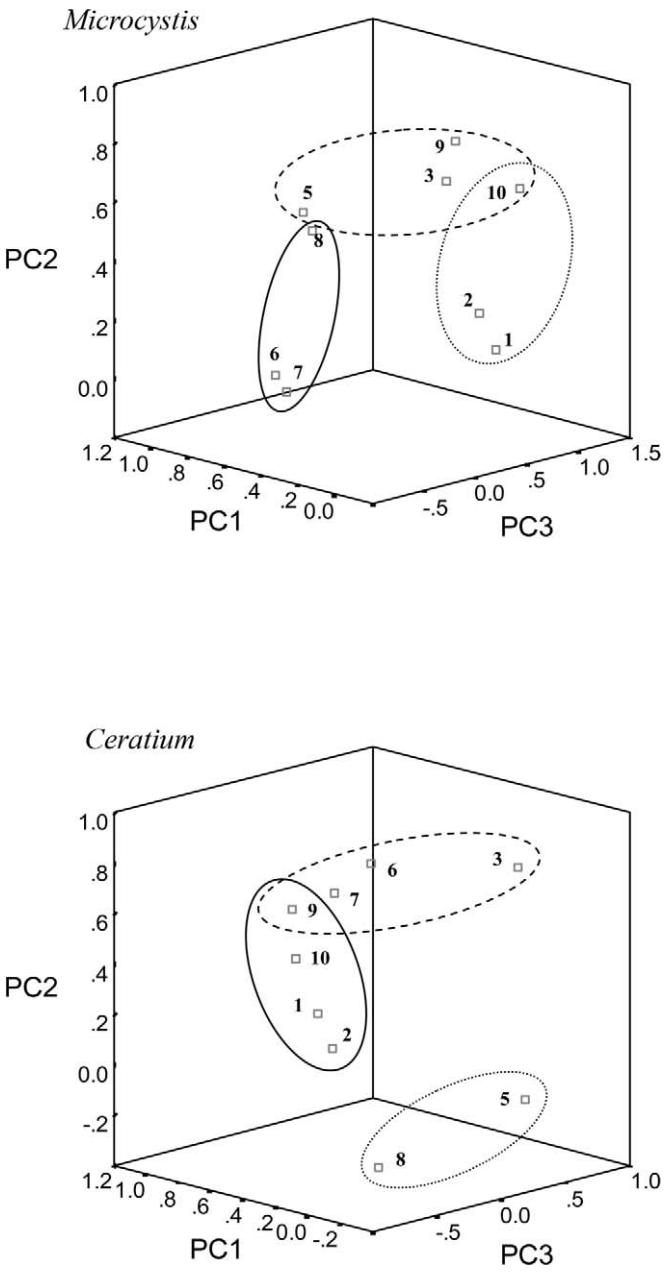

Fig. 5. PCA plot of peak intensities for *Microcystis* and *Ceratium*. For *Microcystis*, PC1 (30% of total variance) consists of bands 6, 7 and 8; PC2 (29%) bands 3, 5, 9, and 10; and PC3 (28%) bands 1, 2 and 10. For *Ceratium*, PC1 (38%) consists of bands 1, 2, 9, 10; PC2 (27%) bands 3, 6, 7 and 9; and PC3 (18%) bands 5 and 8.

Table 5. Comparison of band positions of *Microcystis* and *Ceratium*.

	Microcystis			*Ceratium*			
Band	Mean (cm^{-1})	SD	n	Mean (cm^{-1})	SD	n	Significance
1	3303	7.42	20	3332	49.2	20	ns
2	2929	4.5	20	2919	11.4	18	0.002*
CO_2	*2362*	*1.3*	*20*	*2361*	*1.3*	*19*	
3	1734	0.1	18	1734	1.0	15	
4	1655	3.7	20	1653	0.1	20	
5	1541	2.8	18	1541	0.4	20	
6	1456	2.8	19	1457	0.1	20	
7	1398	5.4	17	1373	3.6	10	0.000*
8	1244	6.3	15	1255	25.5	16	ns
9	1152	2.9	20	1156	1.7	19	
10	1081	2.8	18	1063	1.3	9	0.000*

* Band position significantly different at the 99% probability level; ns, bands separated by >4-cm^{-1} wave numbers but not significantly different. Bands within the 4-cm^{-1} wave-number resolution of the instrument were assumed to be not significantly different.

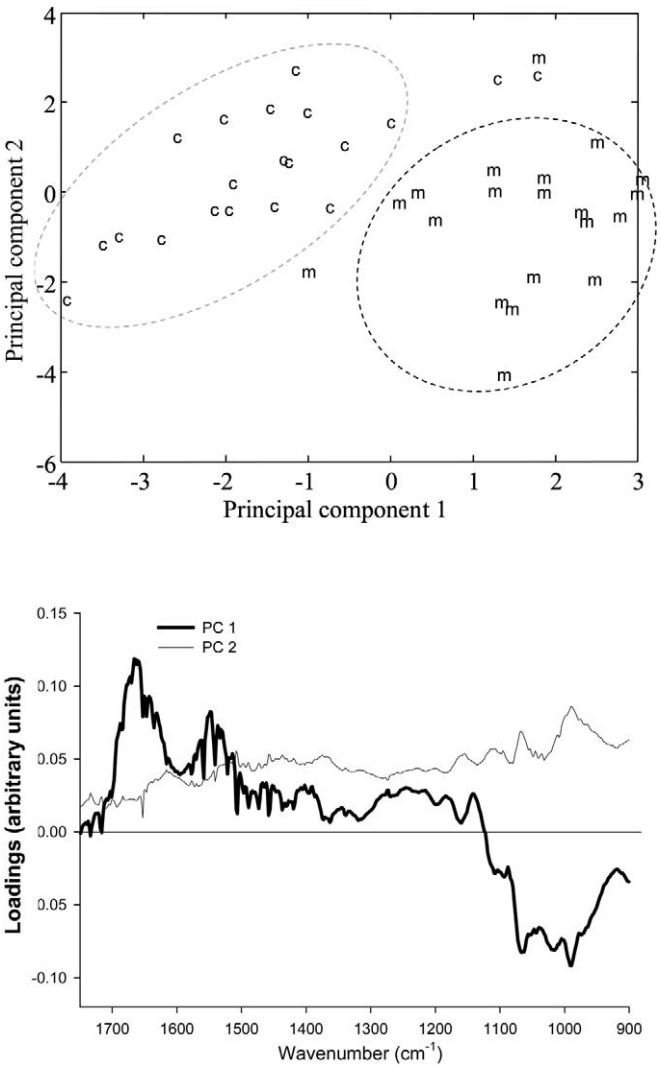

Fig. 6. Scores plot for *Microcystis* and *Ceratium* (top) and (bottom) Loading plot for PC1 and PC2, accounting for 49% and 30% of the variance, respectively.

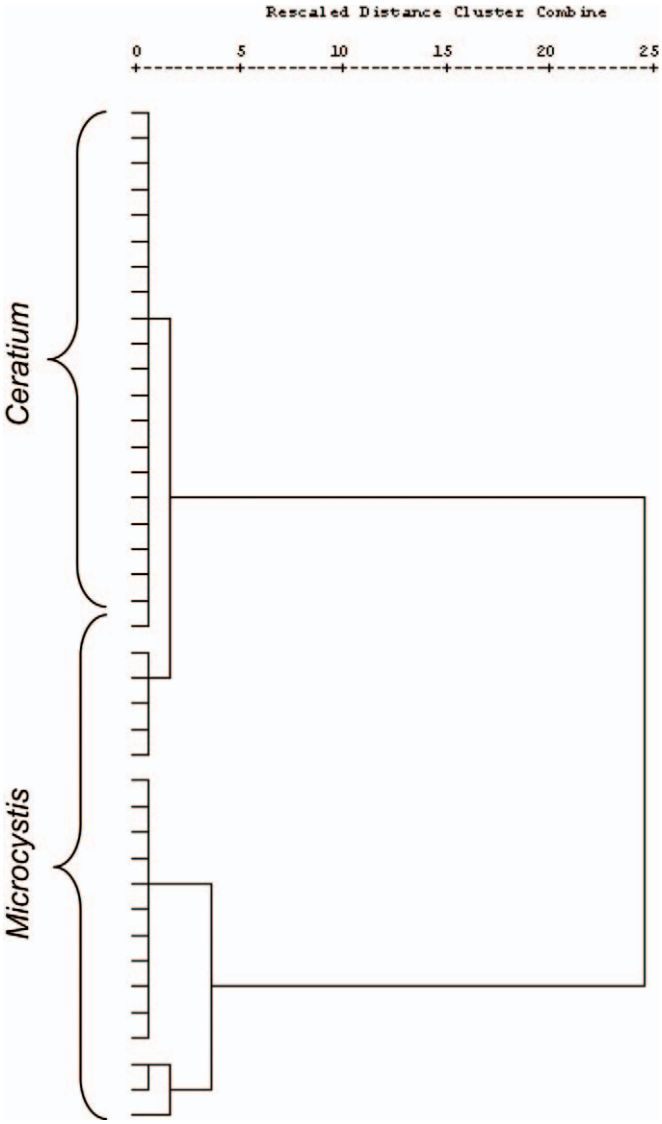

Fig. 7. Dendogram constructed using Ward analysis, using Euclidian distance squared between points. The dendogram was constructed using spectra normalised to amide I, in the 1750–900 cm^{-1}.

spectra present as three separate clusters. Within this dendrogram, only one spectrum associates with the other species.

DISCUSSION

FTIR spectroscopy has been traditionally used in relation to purified biochemicals, including the four major groups of biological macromolecules—nucleic acids (Liquier & Taillandier 1996), proteins (Stuart 1997), lipids (Lewis & McElhaney 1996) and polysaccharides (Brandenberg & Seydel 1996). In recent years, it has also been applied to more complex biological samples and whole organisms, such as bacteria (Naumann *et al.* 1996), fungi (Guibal *et al.* 1995), higher plants (Wetzel *et al.* 1998), tissue culture cells (Holman *et al.* 2000) and microalgae (Sigee *et al.* 2002).

FTIR microspectroscopy of phytoplankton results in complex absorption spectra, analysis of which provides information on both qualitative (band assignments) and quantitative (molecular ratios, population variability, species differentiation) information in freshwater systems (Dean & Sigee 2006).

Band assignments and relationships

Single cells of *Ceratium* and colonies of *Microcystis* generated FTIR spectra with clear bands. The molecular assignments of bands given in Table 2 are based on published data on phytoplankton, noncyanobacterial bacteria and human cells. The problems encountered with identification and interpretation of these bands are similar to those of other whole organisms such as bacteria (Naumann *et al.* 1996) where individual molecular groups contribute to different bands and individual bands are derived from several molecular sources. Information on band assignments can be obtained from correlation and factor analysis of the principal bands, as bands derived from a common source should show a correlation. In this study bands 9 and 10 have been attributed, in both algae, to carbohydrate. Band 9 was positioned at 1150 cm^{-1}, while

the average position of band 10 was at 1081 cm^{-1} for *Microcystis* and 1063 cm^{-1} for *Ceratium.* In some spectra of both algae, bands were also seen at ≈1050 cm^{-1} and ≈1030 cm^{-1}. These band positions match those attributed to the ν(C-O-C) stretching of polysaccharides (Brandenburg & Seydel 1996), which include band positions at 1150, 1078, 1066, 1050 and 1030 cm^{-1}, although Wong *et al.* (1991), Benning *et al.* (2004) and Naumann *et al.* (1996) all attribute a band at 1080 cm^{-1} to the ν(P = O) stretching of nucleic acid. In this study, if band 10 were due to the presence of nucleic acid, then it would be expected to correlate with band 8 (≈1250 cm^{-1}), which is due largely due to υ_{as}(>P = O) stretching. However, no correlation was observed. This suggests that any nucleic acid contribution contributes only weakly to band 10 and that the carbohydrate is indeed the major contributor to this band.

In *Microcystis,* bands 9 and 10 were correlated with bands 1 and 2, while in *Ceratium* band 10 was correlated with 1 and 2. Band 2 (≈2929 cm^{-1}) is usually associated with $\delta as(CH_2)$ of methylene from lipids, while band 3 (1734 cm^{-1}) is derived from the υ(C = O) of ester functional groups primarily from lipids and fatty acids. However, bands 2 and 3 did not show any correlation in either *Microcystis* or *Ceratium,* suggesting that these bands are not derived from a common source. The correlation between bands 2 and 9 and/or 10 suggests that the major contribution to band 2 may be not from lipids but from the strong C-H vibrational modes of carbohydrates. The strong correlation between band 1 and the carbohydrate peaks suggests that it to is derived largely from carbohydrate and not from the usual assignment of water/protein. This is further supported by the factor analysis of the bands, in which bands 1, 2, 9 and/or 10 were grouped together, suggesting that these bands are linked. Further evidence for the assignment of 1 and 2 to carbohydrate comes from the FTIR spectra of starch (Sigee *et al.* 2002), which shows prominent peaks at 2900 cm^{-1} and 3300 cm^{-1}, suggesting that bands 1 and 2 are both due largely due the presence of carbohydrate.

In both algae the close correlation of bands 6 and 7 suggests that they are dominated by the $\delta_{as}(CH_3)$ and $\delta_s(CH_3)$ bending modes of methyl groups of protein. Other workers have stated bands 6 and 7 may have contributions from lipid (Benning *et al.* 2004) and carboxylic acid (Naumann *et al.* 1996; Giordano *et al.* 2001), respectively. However, in this study, the close correlation between the peaks and the lack of correlation with any lipid-derived bands suggest that the contributions of lipids and/or carboxylic acids to these bands are low.

Band 8 (υ_{as}(>P = O)) at a position of 1244 cm^{-1} is likely to have a strong contribution from nucleic acid, but it is likely that this band also has a contribution from the internal storage of polyphosphates, which are important in cyanobacteria such as *Microcystis* (Paerl 1988) and also in dinoflagellates such as *Ceratium* (Pollingher 1988). In *Ceratium,* band 8 was not correlated with any other band, which suggests that it is the only band with a dominant υ_{as}(>P = O) contribution and that, as mentioned above, band 10 (1081 cm^{-1}) is dominated by carbohydrate. Similarly, in *Microcystis* no correlation between bands 8 and 10 were observed, although band 8 did correlate with bands 6 (1456 cm^{-1}) and 7 (1398 cm^{-1}). This is unusual, as bands 6 and 7 are due primarily to $\delta_{as}(CH_3)$ and $\delta_s(CH_3)$ bending of methyl groups. The reason for the correlation between bands 6, 7 and 8 in *Microcystis* is therefore subject to speculation.

Population heterogeneity

Intraspecific variation in band intensity gives a measure of population heterogeneity, indicating how intracellular concentrations of macromolecular components varied between algae taken from the same population.

Band 5 showed the smallest coefficient of variation in both *Microcystis* (8%) and *Ceratium* (10%) The small variation exhibited by this band (amide II) may be a result of the fact that the spectra was normalised to amide I, so that variations in band intensity of amide II are correspondingly reduced. Band 6 and 7 had coefficients of 18% and 20%, respectively, in *Ceratium* and 22% and 28%, respectively, in *Microcystis.* Both these bands are derived largely from protein, and as the spectra is normalised to protein, care has to be taken in interpreting variation in these bands, although, as stated above, other function groups may contribute to variation in these bands, such as lipid (band 6) and carboxylic acid (band 7).

In *Ceratium,* bands 1, 2, 9 and 10 showed the highest variation (CV >30%), with band 10 having a CV of 47%. As discussed earlier, all of these bands are probably derived from carbohydrate, and the high variation in band intensity suggests that the *Ceratium* population exhibits a wide variation in the amount of polysaccharide storage material within the individual cells. Band 8 (≈1250 cm^{-1}), which is commonly attributed to the υ_{as}(>P = O) stretching of the phosphodiester backbone of nucleic acid, had a coefficient of variation of 25% suggesting that *Ceratium* cells showed wide variation in intracellular concentrations of nucleic acid. However, band 8 will also include contributions from any phosphate-containing compound, and it is possible the intracellular stores of phosphorus could contribute to the variation observed in this peak. It is known that *Ceratium* can store excess phosphorus within the cells during bloom development in what is known as 'luxury consumption', which is then utilised when external concentrations become limiting (Serruya & Berman 1975). At the time of sampling, phosphorus concentrations in the lake were undetectable, and it is possible that the *Ceratium* population showed intraspecific heterogeneity in the amount of phosphorus compounds stored within cells. Band 3 is derived from the υ(C = O) stretching mode of ester functional groups, primarily from lipids and fatty acids. This band also showed variation in intensity (CV 26%), suggesting that cells show intraspecific variation in lipid concentration. This may be due to variations in the amount of lipid storage products stored by cells.

Variations in the band intensities were also noted for *Microcystis,* although the variation in bands associated with carbohydrate were less than that observed in *Ceratium,* suggesting that colonies of *Microcystis* were less heterogeneous in terms of their intracellular concentrations of storage products. However, band 3 (lipid) showed the highest CV (36%), suggesting that *Microcystis* colonies have high heterogeneity in the amount of lipid storage products stored by cells. Band 8 again showed a high coefficient of variation (32%), and, as with *Ceratium,* this may be due to variation in the intracellular amount of nucleic acid or due to differences in the cell quotas of P imported during 'luxury consumption'.

Species comparisons

Variations in some band positions were observed between *Microcystis* and *Ceratium,* with bands 1, 2, 7, 8 and 10 differing

by more than the 4 cm^{-1} resolution of the instrument. Some of these bands in *Ceratium* showed high intraspecific variation in position, as exemplified by the high standard deviation in bands 1 and 8. However, only the positions of bands 2 (carbohydrate), 7 (protein) and 10 (carbohydrate) were significantly different at the 99% probability level. These differences may reflect differing intermolecular interactions or molecular structure between the two algal species. For example, the differences in the position of band 10 (1081 cm^{-1} in *Microcystis*, 1063 cm^{-1} in *Ceratium*) may reflect differing molecular structure of the carbohydrate storage products within the two species.

Band intensities also showed differences between the species with all but bands 7, 8 and 9 showing significant differences. Particularly prominent differences were observed the intensity of band 10, with a mean of 0.696 ± 0.197 in *Microcystis* and 1.483 ± 0.698 in *Ceratium*. As discussed above, the wide variation in *Ceratium* suggests wider heterogeneity in the relative concentration of storage products than in *Microcystis*.

As the spectra are normalised to amide I, the higher carbohydrate intensity in *Ceratium* indicates a higher carbohydrate/protein ratio than in *Microcystis*. In another FTIR study (Beardall *et al.* 2001), P-limited cultures of *Phormidium* and *Spaerocystis* showed a higher carbohydrate/protein ratio than those resupplied with orthophosphate. Thus, the higher carbohydrate/protein ratio observed in *Ceratium* may be a response to adverse environmental conditions, for example, the undetectable orthophosphate conditions pertaining at the time of sampling. An FTIR study on *Microcystis* has also shown an increase in the carbohydrate/protein ratio in response to nutrient limitation (Stehfest *et al.* 2005). A low ratio was observed in this study, suggesting that despite low external nutrients, *Microcystis* was not suffering the effects of nutrient depletion to the same extent as *Ceratium*, possibly due to internal stores of P. However, care must be taken in interpreting the data in this way, as Beardall *et al.* (2001) also found that in *Scenedesmus* the carbohydrate/protein ratio actually increased on resupply of phosphorus. The molecular response of algae to adverse growth conditions is therefore likely to be species specific. Furthermore, the difference in the carbohydrate/protein ratio between *Microcystis* and *Ceratium* may not relate to adverse environmental conditions but may simply reflect a difference in C allocation patterns between the algae—under equally optimum growth conditions, the two algae may show differing cellular carbohydrate/protein ratio.

FTIR spectroscopy in phycology

This study demonstrates the ability of FTIR microspectroscopy to determine the molecular compositions of two dominant algal species, *M. aeruginosa* and *C. hirundinella*, within a mixed phytoplankton bloom sample. The ability of FTIR to study the molecular composition of algal cells and colonies makes it a tool with great potential for phycological research. Areas in which the technique may provide important insights include the study of the redistribution of cellular macromolecular components due to environmental stress, for example, the molecular response of individual cells to environmental variations in light and inorganic nutrients (Stehfest *et al.* 2005). This ability to monitor the macromolecular composition of cells may have important applications in monitoring the algal growth response to different external conditions in a controlled environment (algal culture). This study showed a clear distinction, using multivariate techniques, between spectra obtained from algae of different taxonomic groups, and the same techniques have the potential to discriminate between algal species and strains in which visual distinction may be difficult or impossible (e.g. Kansiz *et al.* 1999). Although the use of FTIR in these areas is still in its infancy, it is now beginning to be recognised as a technique with great potential in phycological research.

ACKNOWLEDGEMENTS

DCS and APD gratefully acknowledge ENVIROSYNCH funding (Central Laboratory of Research Councils, UK) for study at The Advanced Light Source Laboratory (Berkeley Campus) and NERC funding (APD) in support of a Studentship. The authors would also like to thank English Nature for permission to carry out sampling at Rostherne Mere and provision of boating facilities.

REFERENCES

BEARDALL J., BERMAN T., HERAUD P., KADIRI M.O., LIGHT B.R., PATTERSON G., ROBERTS S., SULZBERGER B., SAHAN E., UEHLINGER E. & WOOD B. 2001. A comparison of methods for detection of phosphate limitation in microalgae. *Aquatic Sciences* 63: 107–121.

BENNING L.G., PHOENIX V. R., YEE N. & TOBIN M.J. 2004. Molecular characterisation of cyanobacterial silification using synchrotron infrared micro-spectroscopy. *Geocimica et Cosmochimica Acta* 68: 729–741.

BRANDENBURG K. & SEYDEL U. 1996. Fourier transform infrared spectroscopy of cell surface polysaccharides. In: *Infrared spectroscopy of biomolecules* (Ed. by H.H. Mantsch & D. Chapman), pp. 159–202. Wiley, Chichester.

DEAN A.P. & SIGEE D.C. 2006. Molecular heterogeneity in *Aphanizomenon flos-aquae* and *Anabaena flos-aquae* (Cyanophyta): a synchrotron-based Fourier-transform infrared study of lake micro-populations. *European Journal of Phycology* 41: 201–212.

GIORDANO M., KANSIZ M., HERAUD P., BEARDALL J., WOOD B. & MCNAUGHTON D. 2001. Fourier transform infrared spectroscopy as a novel tool to investigate changes in intracellular macromolecular pools in the marine microalga *Chaetoceros muellerii* (Bacillariophyceae). *Journal of Phycology* 37: 271–279.

GUIBAL E., ROULPH C. & LE CLOIREC P. 1995. Infrared spectroscopic study of uranyl biosorption of fungal biomass and materials of biological origin. *Environmental Science and Technology* 29: 2496–2503.

HERAUD P., WOOD B.R., TOBIN M.J., BEARDALL J. & MCNAUGHTON D. 2005. Mapping of nutrient-induced biochemical changes in living algal cells using synchrotron infrared microspectroscopy. *FEMS Microbiology Letters* 249: 219–225.

HOLMAN H.N., MARTIN M.C., BLAKELY E.A., BJORNSTAD K. & MCKINNEY W.R. 2000. IR spectroscopic characteristics of cell cycle and cell death probed by synchrotron radiation based Fourier transform IR spectromicroscopy. *Biopolymers* 57: 329–335.

KANSIZ M., HERAUD P., WOOD B., BURDEN F., BEARDALL J. & MCNAUGHTON D. 1999. Fourier Transform Infrared microspectroscopy and chemometrics as a tool for the discrimination of cyanobacterial strains. *Phytochemistry* 52: 407–417.

KELLER R.J. 1986. *Sigma library of FT-IR spectra*. Sigma Chemical Company, St Louis, MO.

LEWIS R.N. & MCELHANEY R.N. 1996. Fourier transform infrared

spectroscopy in the study of hydrated lipids and lipid bilayer membranes. In: *Infrared spectroscopy of biomolecules* (Ed. by H.H. Mantsch & D. Chapman), pp. 159–202. Wiley, Chichester.

LIQUIER J. & TAILLANDIER E. 1996. Infrared spectroscopy of nucleic acids. In: *Infrared spectroscopy of biomolecules* (Ed. by H.H. Mantsch & D. Chapman), pp. 159–202. Wiley, Chichester.

LITAKER R.W., VANDERSEA M.W., KIBLER S.R., REECE K.S., STOKES N.A., STEIDINGER K.A., MILLIE D.F., BENDIS B.J., PIGG R.J. & TESTER P.A. 2003. Identification of *Pfiesteria piscida* (Dinophyceae) and *Pfiesteria*-like organisms using internal transcribed spacer-specific PCR assays. *Journal of Phycology* 39: 754–761.

MARIEY L., SIGNOLLE J.P., AMIEL C. & TRAVERT J. 2001. Discrimination, classification, identification of microorganisms using FTIR spectroscopy and chemometrics. *Vibrational Spectroscopy* 26: 151–159.

NAUMANN D., SCHULTZ C.P. & HELM D. 1996. What can infrared spectroscopy tell us about the structure and composition of intact bacterial cells In: *Infrared spectroscopy of biomolecules* (Ed. by H.H. Mantsch & D. Chapman), pp. 159–202. Wiley, Chichester.

PAERL H.W. 1988. Growth and reproductive strategies of freshwater blue-green algae (Cyanobacteria). In: *Growth and reproductive strategies of freshwater phytoplankton* (Ed. by C.D. Sandgren), pp. 261–315. Cambridge University Press, Cambridge.

POLLINGHER U. 1988. Freshwater armoured dinoflagellates: growth, reproduction strategies, and population dynamics. In: *Growth and reproductive strategies of freshwater phytoplankton* (Ed. by C.D. Sandgren), pp. 134–174. Cambridge University Press, Cambridge.

REYNOLDS C.S. & JAWORSKI G.H.M. 1978. Enumeration of natural *Microcystis* populations. *British Phycological Journal* 13: 269–277.

SACKSTEDER C. & BARRY B.A. 2001. Fourier transform infrared spectroscopy: a molecular approach to an organismal question. *Journal of Phycology* 37: 197–199.

SERRUYA C. & BERMAN T. 1975. Phosphorus, nitrogen and the growth of algae in Lake Kinneret. *Journal of Phycology* 11: 155–162.

SIGEE D.C. & LEVADO E. 2000. Cell surface elemental composition of *Microcystis aeruginosa*: high-Si and low-Si subpopulations within the water column of a eutrophic lake. *Journal of Plankton Research* 22: 2137–2153.

SIGEE D.C., DEAN A., LEVADO E. & TOBIN M.J. 2002. Fourier-transform infrared spectroscopy of *Pediastrum duplex*: characterization of a micro-population isolated from a eutrophic lake. *European Journal of Phycology* 37: 19–26.

STEHFEST K., TOEPEL J. & WILHELM C. 2005. The application of micro-FTIR spectroscopy to analyze nutrient stress-related changes in biomass composition of phytoplankton algae. *Plant Physiology and Biochemistry* 43: 717–726.

STUART B. 1997. *Biological applications of infrared spectroscopy*. Wiley, Chichester.

VILLAREAL T.A. & LIPSCHULTZ F. 1995. Internal nitrate concentrations in single cells of large phytoplankton from the Sargasso Sea. *Journal of Phycology* 31: 689–696.

WETZEL D.L., EILERT A.J. PIETRZAK L.N. MILLER S.S. & SWEAT J.A. 1998. Ultraspatially-resolved synchrotron infrared microspectroscopy of plant tissue in situ. *Cellular and Molecular Biology* 44: 145–168.

WETZEL R.G. & LIKENS G.E. 2000. *Limnological analyses*. Springer-Verlag, New York.

WILLEN E. 1976. A simplified method of phytoplankton counting. *British Phycological Journal* 11: 265–278.

WONG P.T.T., WONG R.K., CAPUTO T.A., GODWIN T.A. & RIGAS B. 1991. Infrared spectroscopy of exfoliated human cervical cells: evidence of extensive structural changes during carcinogenesis. *Proceedings of the National Academy of Sciences* 88: 10988–10992.

Received 5 April 2006; accepted 9 October 2006
Associate editor: J. Beardall